The Mechanical Behavior of Ceramic/Metal Laminate Under Thermal Shock

Dov Sherman and Doron Schlumm
Department of Materials Engineering
Technion-Israel Institute of Technology
Haifa 32000, Israel

SUMMARY: A new material system for applications involving thermal shock is proposed. The system consists of thin layers of ceramics and thinner metallic interlayers. In this study, a ceramic/metal laminate was constructed from Coor's ADS96R thin plates alternating with thinner Wesgo Cusil ABA interlayer foils and joined in active brazing. Square shaped laminated plates were quenched in room temperature distilled water from initial temperature of 600^{o}C.

The basic features of this architecture are described. The dominant behavior was the absence of interaction between the biaxial cracking mechanisms in an individual layer, and localization of the damage to those layers experienced sufficient tensile stresses. The result was a dramatic increase of the residual strength after thermal shock. In addition, R-curve behavior upon mechanical loading due to plastic deformation of the metallic interlayer was observed. The effect of the metallic interlayers' thickness is described as well.

1. INTRODUCTION

When monolithic ceramics are subjected to high heat transfer or rapid changes in temperature, damage in the form of cracks occurs due to high tensile stresses, inherent low fracture toughness, and the presence of processing flaws [1-4]. The critical temperature**,** ΔT_C, is usually defined [4] as the temperature difference between the maximum temperature of the specimen (or even the furnace temperature) and the temperature of the quenched media prior to cracking. This critical temperature as a function of specimen thickness for several ceramics quenched in water was determined experimentally [4], and demonstrated increased critical thermal difference as the specimen's thickness reduced.

While some materials, such as ordinary glass, can take a temperature shock of only 80^{o}C before cracks initiate, others, like Silicon Nitride [4] can withstand sudden changes of more than 600^{o}C. Therefore monolithic ceramics are not sufficiently strong to serve at high temperatures and in harsh environments when thermal shock must be taken into account [5]. Hence, a combination of materials and a different architecture are needed.

We propose a new material architecture with a view to increasing the maximum difference in temperature that ceramics can withstand and still maintain structural integrity and strength. The new architecture consists of thin ceramic layers alternating with thinner metallic interlayers. In this system, the ceramic is the high melting point constituent, possessing high stiffness, high wear and fatigue resistance, and able to maintain these properties in a corrosive environment and at elevated temperatures. The metal interlayers provide the needed compliance, ductility, and toughness. The interface should be strong enough to prevent crack deflection and disintegration of the material system. In this contribution we report the basic mechanical behavior of the new architecture.

2. EXPERIMENTAL PROGRAM

2.1 Constituents and laminate

The ceramic constituent in this investigation was Coor's ADS96R nominally 370 μm thick alumina plates, the metallic constituent - thin Wesgo Cusil ABA (63 wt % Ag, 1.75 Ti, and bal. Cu.) sheets (**Table 1**). The liquidus of the brazed alloy is 780^{o}C, the solidus 815^{o}C. The alumina layers and metallic interlayers were joined by brazing, a low cost and simple processing route (viz. relatively low temperature, pressure, and time requirements). No special surface treatment was used, aside from cleaning the materials in an ultrasonic acetone bath. The specimens were put under low pressure (0.15 MPa), applied by a solid fixture at room temperature. Brazing was carried out under vacuum of 10^{-5} Torr, at a maximum temperature of 845^{0}C, held for 10 minutes to achieve good bonding. The brazing process of the current system has lately been extensively studied [6-8], as have the brittle product layers generated during processing.

Table 1. The mechanical and physical properties of the constituents.

	E	ν	σ_Y	σ_{UTS}	ε_{UTS}	α	k	ρ
	GPa	-	MPa	MPa	%	$^{o}C^{-1}$	W/(m*C)	g/cm^3
ADS96R	320	.21	320	-	-	8.3	22	3.9
Cusil ABA	83	-	271	346	20	18.5	180	9.8

Two types of laminates were constructed. The first (designated 9A8C) was constructed from 9 alumina layers and 8 metallic interlayers, the average thickness of the metallic interlayers was 30 μm, the second (8A7C) was constructed from 8 alumina plates and 7 metallic interlayers with average thickness of 90 μm. The total thickness of both laminates was 3.6 mm, and the specimens were square shaped with a gage area of 25x25 mm^2.

2.2. Thermal shock conditions

A special apparatus for thermal shock testing was designed and built. It consisted of an open furnace, a special stage which kept the specimen horizontal during quenching (**Fig. 1a**), and a piston pushing the specimens towards a small container of distilled water such that only the bottom surface of the specimen experienced the thermal shock. Two thermocouples, measuring the temperatures of the top and the bottom surfaces of the specimens (**Fig. 1b**) at a rate of 17 Hz, were connected to a PC for data recording. The thermocouples were k-type, 0.15 mm in diameter. The tip of each thermocouple was ground to a hemispherical shape and attached to the specimen using Cerambond® cement. The total volume of the cement and the tip did not exceed 2 mm^3, to minimize any influence on the temperature measurements. Laminated specimens were quenched in water, from initial temperatures of 600^{o}C (below solidus). To avoid cooling of the top surface of the specimens due to turbulence of the water during quenching, and to prevent irrelevant cracking at the specimen's edges, four thin alumina plates were bonded to the specimen's edges by Cerambond® (Fig. 1b). This ensured that the quenched specimens could as closely as possible be considered as an infinite plate. The limited strength of the bond, the porosity in it, and the low amount of bond that was used prevented any significant constraint of the tested specimens.

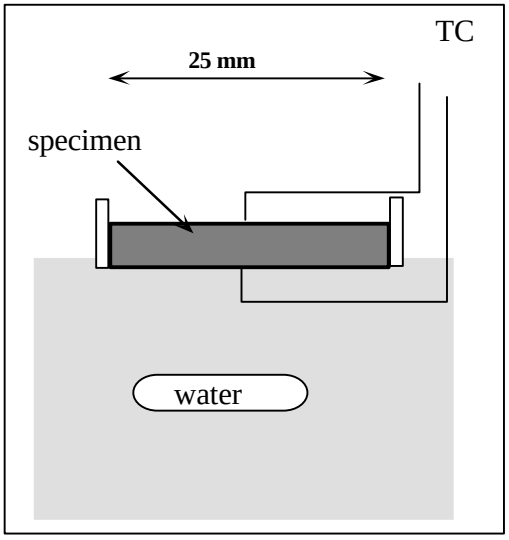

Fig. 1a. Schematic presentation of the specimen at quenching

Fig. 1b. The thermal shock apparatus

2.3 Evaluation of the laminate after thermal shock

After quenching, the laminated plates were cut to form bending beams and were tested under three (3PB) and four (4PB) point bending (outer span of 20 mm). The beam width was kept to 3.5 mm. Quenched specimens and those that were also mechanically loaded were analyzed by HRSEM.

3. RESULTS AND DISCUSSION

3.1 The mechanical behavior of the laminate

The residual stresses after brazing are difficult to analyze when constrained thin layers are involved. Based on the linear elastic behavior of the metallic interlayer during cooling down, and using the mechanical and thermal properties shown in **Table 1**, the room temperature residual stresses in the alumina layers and in the metallic interlayers are shown in **Table 2**. These results set the upper bounds for the stresses, since limited stress relaxation due to dislocation movement in constrained layers is expected [9].The calculated tensile stresses in the metallic interlayers were about 3 times the tensile strength, resulting from the high hydrostatic stresses within these constrained layers. The load-deflection curve of the laminate under 3PB exhibit brittle behavior with no energy dissipating feature.

3.2 Mechanical behavior of the laminate under thermal shock

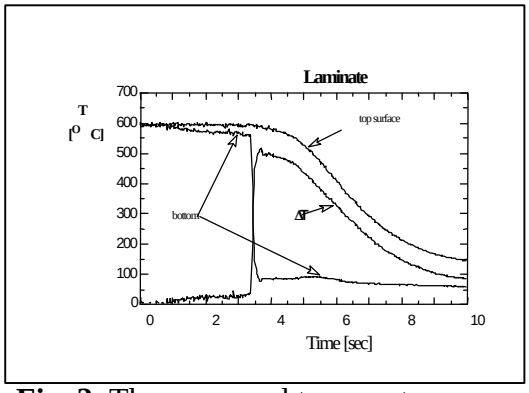

Fig. 2. The measured temperatures.

A t ypical temperature-time relationship at the quenched from an initial temperature of 600^{O}C, and the differences between these temperatures, (designated ΔT_{mech}) are shown in **Fig. 2**. A typical network of cracks was seen in the outer alumina layer after thermal shock, see below. However, the compressive stresses in the alumina layers made a complete identification of the cracks difficult, even by microscopic analysis.

HRSEM micrographs revealed a limited crack deflection and microcracks at the interface between the metallic interlayers and the product layers were observed, rather than at the interface between the product layers and the alumina layers. No interaction between the cracking mechanisms in a ceramic layer with those in an adjacent ceramic layer was evident, which indicated that the cracking mechanisms in each ceramic layer is an *independent event* associated with the maximum tensile stresses in that layer. If the tensile stresses in a layer are lower than the ultimate tensile stresses of the layer, it remains completely undamaged. The statistical nature of the strength of ceramics, by means of Weibull Statistics should be taken into account when a rigorous analysis of the behavior is to be considered.
Mechanical tests of bending beams that were cut from laminated specimen before and after quenching of both the 9A8C and 8A7C laminates are shown in **Fig. 3a and b**, respectively.

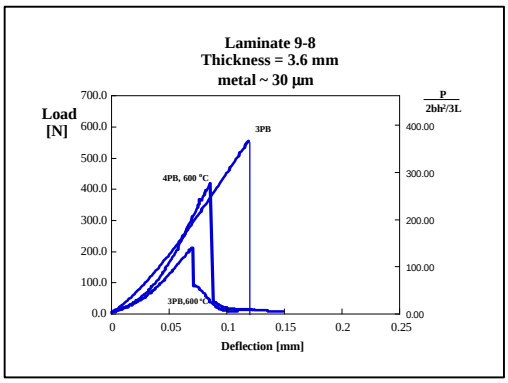

Fig. 3a. Load-deflection of 9A8C laminate

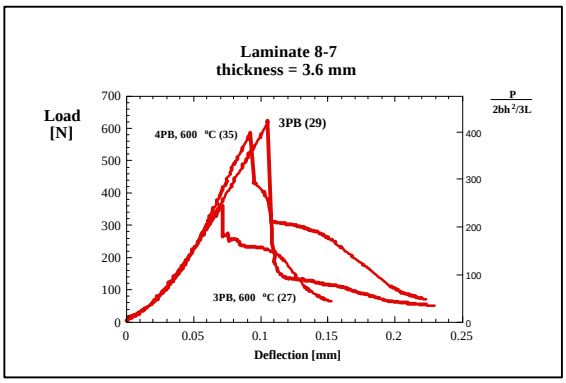

Fig. 3b. Load-deflection of 8A7C laminate.

The results of the mechanical tests are summarized in **Table 2**, where the maximum loads and normalized loads, $P/(2bh^2/3L)$, are presented.

Table 2. The thermal residual stresses, loads and normalized loads to fracture before and after thermal shock of two laminates.

	Res. Str. [MPa]		Failure loads [N]			Norm. loads [MPa]		
			before	after		before	after	
	alumina	metal	3PB	3PB	4PB	3PB	3PB	4PB
9C8M	-72.4	886	560	210	419	330	151	148
8C7M	-181.8	854	624	372	587	423	267	208

The maximum load to failure of monolithic alumina specimen with the same geometry and testing condition, was found to be 20 N, indicating over an order of magnitude increased load to failure of the 9C8M laminate, and larger increase for the 8C7M laminate. Furthermore, the quenched laminate exhibited R-curve behavior, while the pristine laminate was deformed in a completely brittle manner.
An HRSEM analysis of the deformation mechanisms of the metallic interlayers of a 9C8M laminate quenched from 600^{o}C is shown in **Figs. 4**. The first micrographs (**Fig. 4a**) is of the first metallic interlayer from the quenched surface, reveals the plastic deformation after a large crack opening. The subsequent micrographs, **Figs. 4b to 4h,** represent the evolution of the deformation in the subsequent metallic interlayers. The strong interface is evident in all these figures. Microcracking at the highly strained and constrained metallic interlayers were observed.

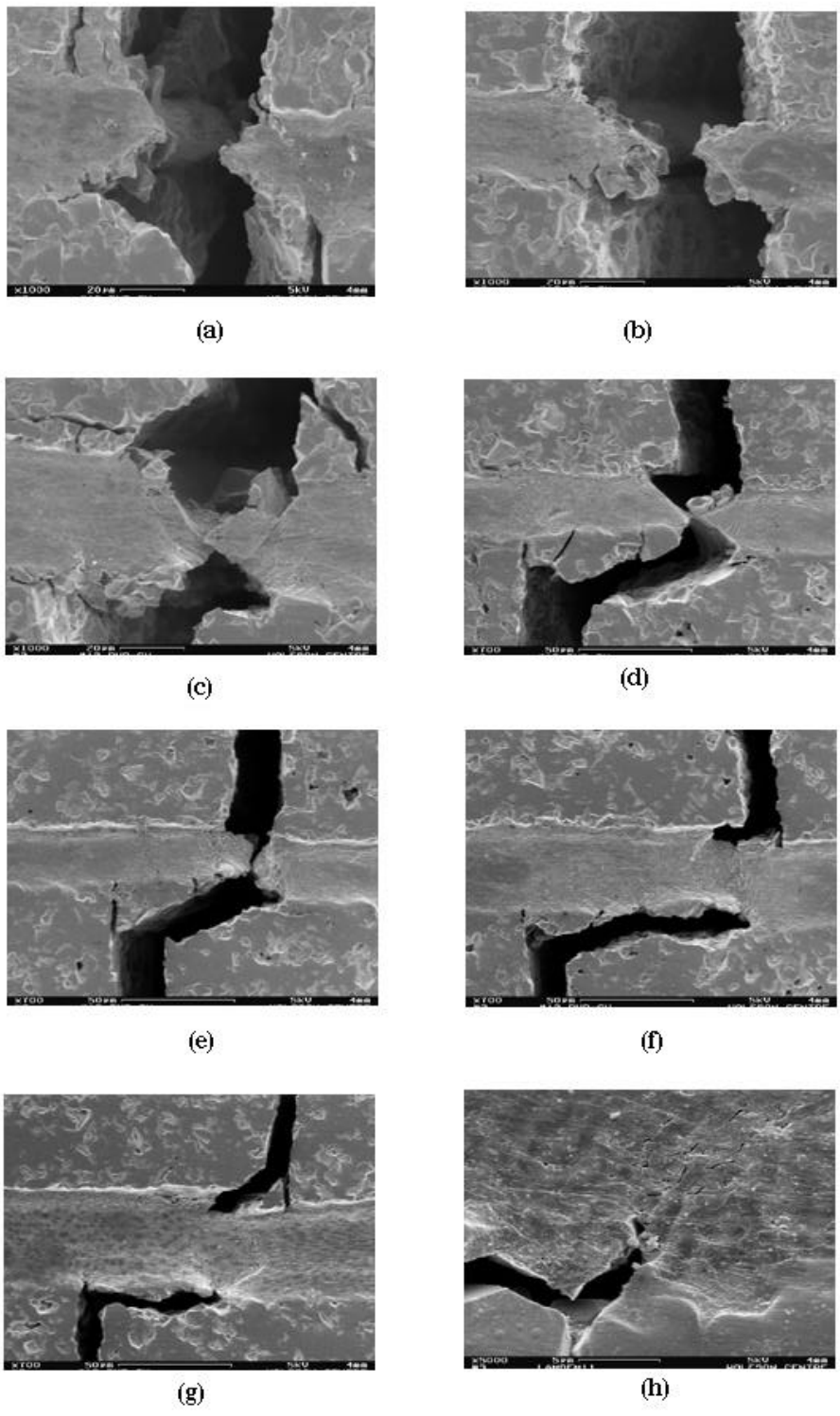

Fig. 4. The progressive plastic deformation in the metallic layers of the 9C8M laminate.

The R-curve behavior under mechanical loading obtained in quenched laminates was the result of the increased volume of the metallic interlayers subjected to plastic deformation due to the small crack deflection of cracks at the metal interlayers/product layer interface, **Figs. 4**.

Acknowledgment: This research was funded by the UK-Israel Science and Technology Research Fund. The assistance of the Wolfson Centre for Interface Studies with the HRSEM micrographs is also acknowledged.

REFERENCES

1. D.P.H. Hasselman, J. Am. Ceram. Soc. **52**, 1955, p. 600.
2. Zhi-He Jin and Y.W. Mai, J. Am. Ceram. Soc. **78**, 1995, p. 1873.
3. N. Claussen and D.P.H. Hasselman, in Thermal Stresses in Severe Environments, D.P.H. Hasselman and R. A. Heller (eds), Plenum Publishing Corp., 1980, p. 381.
4. P.F. Becher and W.H. Warwick, NATO ASI Series, Series E: Applied Sci. -Vol. 241, G. A. Schneider and G. Petzow (edts.), Kluwer Academic Publishers, 1993, p 37.
5. K. Upadhya et. al., J. Am. Ceram. Soc. Bul., December 1997, p 51.
6. C. H. Cho and Jin Yu, Scripta Met., **26**, 1990, p. 1737.
7. M. Naka, K. Sahpath, I. Okamoto and Y. Arata, Mat. Sci. and Eng., **98**, 1988, p. 407.
8. D. Sherman, Materials Letters, **33**, 1998, p. 255.
9. A. G. Evans and J. W. Hutchinson, Acta Metall. mater. **43**, 2507 (1995).
10. D. Sherman and D. Schlumm, Submittd (1998).